Proceedings of PVP2006-ICPVT-11
2006 ASME Pressure Vessels and Piping Division Conference
July 23-27, 2006, Vancoucer, BC, Canada

PVP2006-ICPVT-11-93847

CYLINDER WAKE DYNAMICS IN THE PRESENCE OF STREAM-WISE HARMONIC FORCING

M.Rodriguez, N.W. Mureithi
BWC/AECL/NSERC Chair of Fluid-Structure interaction
Department of Mechanical Engineering
École Polytechnique
Box 6079, Succ. Centre-Ville, Montréal, QC, Canada, H3C 3A7

ABSTRACT

The vortex wake flow dynamics downstream of a cylinder undergoing streamwise harmonic ($f_e/f_s=1$) forced oscillations has been investigated numerically using a CFD code for Re=1000. The steady-state of the wake flow has been analysed considering the amplitude of oscillations as a perturbation parameter.

The resulting dynamics of the fluid lift and drag forces acting on the cylinder have been linked to the different vortex wake modes observed downstream of the cylinder. Forced oscillations lead to periodic, quasi-periodic and chaotic responses depending on the amplitude of oscillation of the cylinder. Different vortex wake patterns or modes (including 2S, P+S and S modes) have also been identified and described. Symmetry related bifurcations both in the computed fluid force dynamics as well as in the vortex wake patterns were identified.

The key role played by spatio-temporal symmetry in the interaction between the wake flow and the oscillating cylinder has been elucidated by a Proper Orthogonal Decomposition (POD) of the wake velocity field. Symmetric and antisymmetric spatio-temporal modes were identified and bifurcations in the wake flow were explained in terms of mode interactions in the wake.

INTRODUCTION

Investigating vortex induced vibrations of a cylinder or harmonic forced oscillations of a cylinder, researchers showed the key role of the vortex configuration in the wake. Defining a terminology describing vortex wake modes in term of shed single vortex or pair of vortices, Williamson & Roshko (1988) compiled a map of vortex wake modes resulting from transverse induced vibrations as a function of the amplitude and frequency of the oscillating cylinder. Interaction between the cylinder motion and the wake is a complex feedback phenomenon in which the symmetry relationship between the unforced wake and the cylinder motion in terms of combined reflection and translation-periodicity seems to play a key role. Ongören & Rockwell (1988) experimentally observed the effect of the frequency and the direction of forced oscillation on the vortex wake structure. Mureithi et al. (2002, 2005) showed the effect of interaction deriving mode amplitude interaction equations between the wake and the cylinder oscillations using symmetry equivariant bifurcation theory. Changes in the wake symmetry induced by increased forcing such as period doubling or symmetry breaking in the cylinder's wake in the case of streamwise harmonic forcing were predicted.

Using numerical simulation as a key tool to easily investigate the dynamics of the wake under streamwise harmonic forcing (frequency ratio equal to unity) at Re=1000, the two dimensional flow is analysed in terms of vortex wakes modes, identified with the vorticity field, depending the amplitude of oscillations. Lift and drag force time evolutions are also analysed in terms of periodicity, symmetry and lock-in with the cylinder motion. Supposing mode interaction in the wake, the flow is analysed using Proper Orthogonal Decomposition (POD) in order to extract the main spatio-temporal modes in the wake flow to explain the effect of the controlled forcing on the wake flow structure and the resulting vortex wake modes.

Copyright © 2006 by ASME

CFD COMPUTATIONS

Numerical simulations were performed using the CFD code Fluent. A rectangular domain around a circular cylinder, having a diameter *D*, was generated using the Fluent preprocessor Gambit. Computation domain boundaries are 15*D* upstream, 40*D* downstream and 20*D* on the lateral sides. Special care was required to avoid the influence of boundaries. To solve the Navier-Stokes equations, Fluent uses a standard path in finite volume method. A second order upwind scheme is used to obtain the face values needed for the integral computations. A second order temporal integration is performed during the simulations.

The forced cylinder inflow oscillation is given by

$$x(t) = \rho A \sin \omega t \, \vec{e}_x . \tag{1}$$

To account for the non-Galilean reference frame, the following time-dependent inertial force on the complete flow field is introduced,

$$F_I(t) = \rho A \omega^2 \sin \omega t \, \vec{e}_x \tag{2}$$

Appropriate boundary conditions are employed for the non-Galilean cylinder reference frame simulations. Inflow and lateral sides' boundary conditions are:

$$\begin{aligned} u &= U - A\omega \cos \omega t, \\ v &= 0, \end{aligned} \tag{3}$$

while the outflow boundary conditions are:

$$u = \mathit{free} \text{ and } v = \mathit{free} \tag{4}$$

The time dependent conditions are input to Fluent by defining an UDF (user defined function). Simulations are all carried out for a flow at Re=1000. At this Reynolds number the cylinder wake is three dimensional and turbulent. As shown in Blevins (1990), the span wise correlation for a rigid cylinder vibrating at resonance with vortex shedding increases with the amplitude of oscillations. So, as justified in Blackburn & Henderson (1999), the two dimensional harmonic forcing of the cylinder will produce flows more two dimensional than the fixed cylinder wake. Furthermore, the stochastic nature of turbulent three dimensional flows is not believed to be important vis-à-vis the primarily two dimensional mechanisms governing the fluid-structure interactions considered here.

Validation and accuracy of results

Test cases and verification of the accuracy of results have already been presented in Mureithi & Rodriguez (2005). Only a recapitulation of the validation is presented. The case of the fixed cylinder has been used in order to validate the numerical model and the accuracy of simulation results. The resulting mesh has the following characteristics: 260 000 elements (corresponding to 125 000 nodes and 135 000 cells). Special care was required in meshing of the cylinder boundary layer which is excited by the oscillating cylinder. The time step has been chosen to capture the dynamics of the wake. It is equal to 1/100 of the supposed vortex shedding period (which coincides with the cylinder frequency of oscillation when forcing is applied). The accuracy of our results has been verified by comparing our drag and lift coefficients (respectively C_D, C_L) and Strouhal number (St) values to some experimental and numerical data, as shown in Table 1.

The Strouhal number (St=0.2366) is high compared to experimental results but the value is reasonable with regard to other two dimensional simulations. The drag coefficient $\left(C_{D,r.m.s} = 1.3563, \bar{C}_D = 1.2691\right)$ is larger than in Roshko's (1954) experiments. This can be explained by the absence of turbulence modelling in our simulation. The r.m.s lift coefficient results are close to Hua's (2005) results; comparison is made between our r.m.s value and Hua's minimum and maximum C_L.

Re = 1000	St	C_D	C_L
Present results *computation*	0.237	1.2671~1.3563	0.8480
Hua et al (2005) *computation*	0.239	1.489±0.198	±1.378
Roshko (1954) *experiments*	0.21	1.2	

Table 1.Summary of present results compared to other computational and experimental data.

Figure 1 shows the Von Karman wake downstream the cylinder. The change in the configuration of vortices beyond ten diameters downstream the cylinder is in agreement with experimental observations (see Van dyke (1982)) and the computational results of Hua et al. (2005).

Figure 1. Vorticity field (s^{-1}) past a fixed cylinder

FORCING AT RE=1000

The effects of stream-wise forcing on the cylinder wake flow have been investigated using the amplitude of forced oscillations as a perturbation parameter. The maximum amplitude simulated here was chosen to be of the same order as the finding of Nishihira et al. (2005) who evaluated the maximum peak amplitude of in-line vortex induced vibration at 0.2*D*. Simulations have been carried out using the von Karman wake of the fixed cylinder as an initial condition from which the cylinder starts to oscillate. Simulations have been

Copyright © 2006 by ASME

carried out for 10000 time steps. Only the last 5000 time steps were used in the analysis. Our results presented focus on the emergence of periodic dynamics in the vortex shedding but quasi harmonic and chaotic responses of the wake flow to the forced oscillations are also described. Presented results included the effect of the forcing on the lift frequency (or Strouhal number), descriptions of the fluid force trajectory along the cylinder path and the vortex wake dynamics. A Proper Orthogonal Decomposition of the wake velocity profile is also presented.

1. Lift frequency effect

For each simulation, the steady state lift frequency (or the last 5000 time steps in case of non periodic response) is analyzed in term of main frequency found in the frequency decomposition as a function of the amplitude of oscillation. The evolution of the Strouhal number with increasing amplitude follows a parabolic type decreasing curve up to a value equal to half the Strouhal number of the fixed cylinder (Figure 2). This value is reached at *A/D* equal to 0.15. The Strouhal number remains constant up to *A/D*=0.4. The streamwise perturbation of the von Karman wake due to the oscillations of the cylinder results in a strong period doubling clearly identified while the lift is also enhanced (not shown). Further insight into the effect of the perturbations is gained by analyzing the dynamics of the fluid force acting on the cylinder as discussed next.

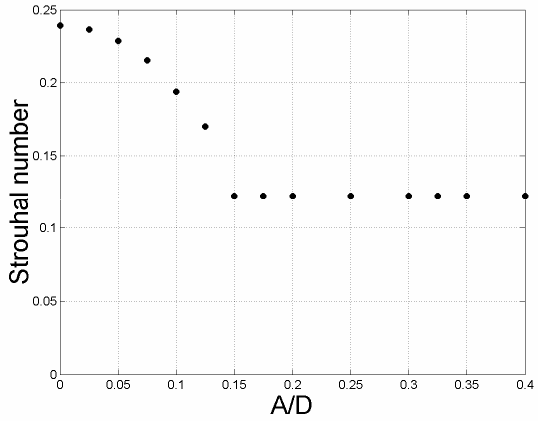

Figure 2. Strouhal number as a function of A/D.

2. Fluid force trajectory

A series of transitions has been observed in the fluid force acting on the cylinder as the amplitude of oscillations is increased. The sinusoidal acceleration of the cylinder controls the boundary layer and the dynamics of its successive separations and reattachments. As the magnitude of the acceleration of the cylinder increases with the amplitude of oscillations, increasing the perturbation parameter (A) affects the roll up of the shear layers. To explain the effect of the cylinder oscillations, the steady state dynamics of the fluid forces are presented in this section.

Time evolution of the lift and drag coefficients as well as frequency decomposition of the lift time evolution shows the temporal periodicity of the dynamics. Three dimensional graphics, representing the evolution of the fluid force as a function of the cylinder position, give the "trajectory" of the fluid force and shows its repeatability and its possible lock-on to the cylinder oscillations. Evolution of the drag and the lift forces as a function of the cylinder position underlines the lock-on of fluid forces to the cylinder motion and the influence of its acceleration on the fluid force dynamics. Ranges of similar behaviour of the fluid force were identified and are described here.

The first range is found up to *A/D*=0.075. The results shown here are for *A/D*=0.05. A beating phenomenon is observed in the drag and lift coefficient time evolutions (Figure 3(a),(b)). The existence of a second frequency is confirmed by the frequency decomposition of the lift coefficient time evolution in Figure 3(c). As the amplitude of oscillation is increased, the beating phenomenon of the drag coefficient is enhanced. The quasi periodicity effect evolves in such a way that the main frequency is a decreasing function of the amplitude of oscillations (Figure 2). A transition in the fluid force dynamics appears for *A/D* above 0.075.

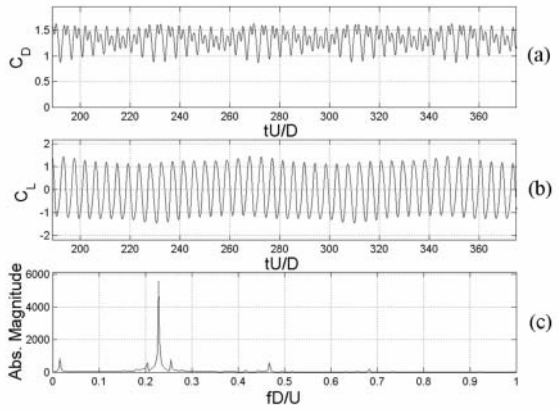

Figure 3. (a) Drag, (b) lift coefficient time evolution and (c) lift coefficient frequency decomposition for A/D=0.05.

Nishira et al. (2005) measured the fluid forces acting on a cylinder under forced oscillations for several reduced velocities (V_r=1 *to* 6) and *A/D*=0.05 at *Re*=3.4.10^4. At V_r=5, a beating phenomenon was observed in the lift time evolution, but at this Reynolds number, the r.m.s lift is small (in experiments C_L*(r.m.s)*=0.064 was found) compared with the case of *Re*=1000. Note also that the present numerical results simulate the case of a massless, undamped rigid cylinder. Thus instead of the common beating phenomenon, differences in the results may be expected.

A second state is identified for 0.1<*A/D*<0.125. The results shown in Figure 4 are for *A/D*=0.125. A chaotic

Copyright © 2006 by ASME

behaviour of the lift and the drag coefficients time evolutions is observed (Figure 4(a),(b)). This is confirmed by the lift coefficient frequency decomposition in Figure 4(c). Applying a Poincaré map reduction (not shown) does not reveal any clear periodicity of the force.

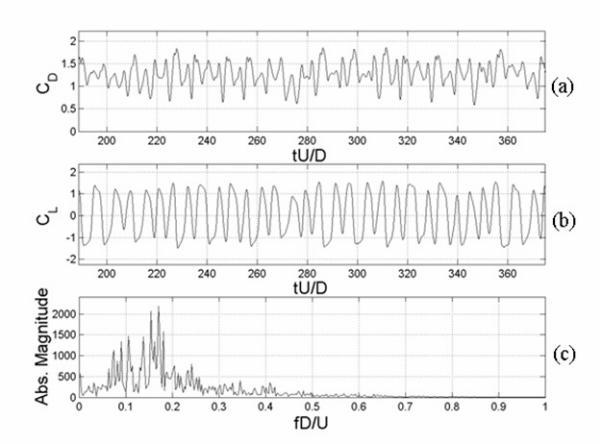

Figure 4. (a) Drag, (b) lift coefficient time evolution and (c) lift coefficient frequency decomposition for A/D=0.125.

For *A/D*=0.15, drawing the fluid force along the cylinder path results in unique trajectory as shown in Figure 5.(Note: In Figures 5-7, both a 3D plot (dark line) as well as 2D projections on the three planes are shown). This confirms the periodicity and reproducibility of the fluid force at every oscillation of the cylinder once the steady state is reached. A frequency decomposition of the lift coefficient time evolution confirms this result. For *A/D*=0.15, the period doubling of the fluid force is accomplished (Figure 2) and the fluid force stabilizes from a chaotic state to a periodic one.

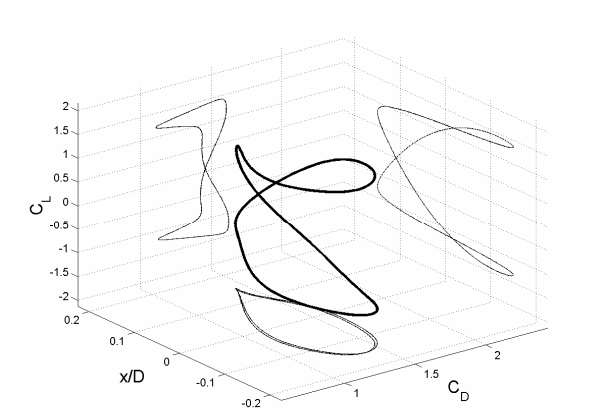

Figure 5. Force trajectory along the cylinder path for A/D=0.15.

For 0.175<*A/D*<0.325, the periodic trajectory in the three dimensional space is clearly asymmetric (Figure 6 and its projection on the planes). Results discussed here are for *A/D*=0.25. The force destabilizes via reflection-symmetry breaking. The fluid force trajectory projected on the *(x/D, C_D)* plane (Figure 6) shows two distinct trajectories for the drag depending on the cycle of oscillation considered.

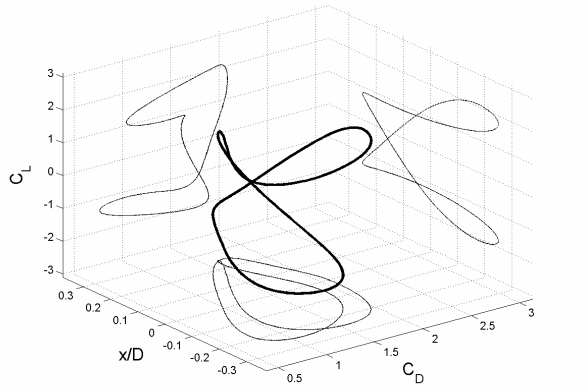

Figure6. Force trajectory along the cylinder path for A/D=0.25.

For *A/D*=0.35, transition in the fluid force leads to a regain of symmetry in the wake dynamics. The lift force still has a primary frequency at half the fixed cylinder vortex shedding frequency (Figure 2) but now the force trajectory is symmetric, thus only a single curve is traced in the *(x,C_D)* plane (on the projected plane Figure 7). At each consecutive cycle the lift time evolution is the opposite that of the preceding cycle while the drag time evolution is the same.

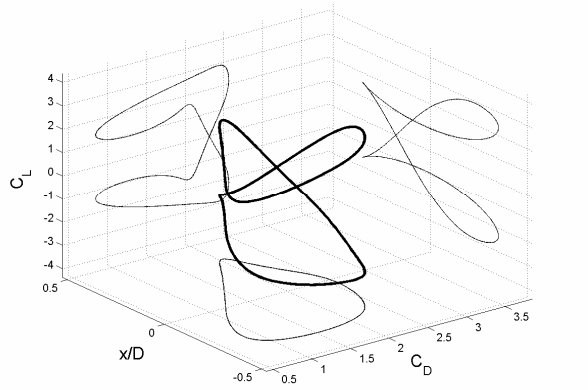

Figure 7. Force trajectory along the cylinder path for A/D=0.35.

From *A/D*=0.15, the fluid force dynamics reached a periodic state. Three ranges are distinguished each one having a proper symmetry. At 0.15, the fluid force has reached a period doubling but even if it is close, the fluid force trajectory is not exactly symmetric from one cycle to the next. From *A/D*=0.175 to 0.3, the period doubling of the fluid force trajectory is still present and the symmetry breaking evident. At *A/D*=0.3, a regain of reflection symmetry in the fluid is

Copyright © 2006 by ASME

reached giving complete period doubling from the non perturbed Karman wake. From a periodic fluid force oscillating at the vortex shedding frequency, the fluid force now oscillates at twice the non perturbed Karman vortex shedding frequency.

As fluid force oscillation is clearly connected to the dynamics of the shear layers and thus vortex shedding, the vortex wake modes are described next in order to explain the symmetry transitions in the fluid force dynamics.

3. Vortex wake modes

Four distinct ranges exhibiting quasi-periodic or periodic dynamics were observed. It is now shown that each one corresponds to a specific vortex wake mode. Using Williamson and Roshko's (1988) terminology, wake structures are described. In the figures below, clockwise vortices appear in grey while counterclockwise vortices appear in black. As the amplitude of oscillation is the controlled parameter, changes in the vortex wake are explained with respect to the increasing of the perturbation parameter. Increase of the amplitude of oscillation increases in turn the acceleration of the cylinder which affects the roll up of the shear layers and the formation of vortices.

For low forcing amplitudes, in the range where quasi periodic dynamics are established for the fluid force, the vortex wake mode is close to the vortex shedding mode of the fixed cylinder. The wake has a *2S* configuration slightly perturbed transversely which explains the beating phenomenon exhibited in the fluid force dynamics. This wake mode is in agreement with the wake pattern found for *A/D=0.05* and V_r=5 in the experiments of Nishihira et al. (2005) who carried out forced in line oscillations of a cylinder at $Re=1.7.10^4$.

For *A/D*=0.15, Figure 8, the vortex wake mode is close to symmetric with a period double that of the non-perturbed vortex shedding. The vortex wake not too far from the cylinder is identified as a *S* mode in Williamson & Roshko's (1988) terminology. The coalescence of the pair of vortices shed every cycle of cylinder oscillations thus results in a *S* vortex wake.

Figure 8. Vorticity field (s^{-1}) past an oscillating cylinder in the stream wise direction, A/D=0.15.

For 0.175<*A/D*<0.325, results are presented in Figure 9. For *A/D*=0.25, symmetry breaking of the fluid force trajectory and the vortex wake occurs. The increase of the roll up of the shear layer induces the formation of more vortices in an asymmetric vortex shedding process which results in a *P+S* configuration a few diameters downstream in the wake. A symmetric perturbation thus induces a symmetry breaking in the wake flow. Simulations starting from different initial conditions show that the wake can destabilize into one of two asymmetric *P+S* configurations without any preference. These configurations are mirror images relative to an axis parallel to the flow and passing through the cylinder centre.

Figure 9. Vorticity field (s^{-1}) past an oscillating cylinder in the stream-wise direction, A/D=0.25.

Experimental tests of forced in-line oscillations of a cylinder at *Re=190* by Griffin & Ramberg (1974) found a *P+S* mode for *A/D=0.24* and a forcing frequency 1.88 times the Strouhal frequency of the fixed cylinder. The *P+S* mode was explained as a consequence of the amplitude of oscillations "reaching a value too great to permit alternating pattern to continue". Blackburn & Henderson (1999) also found a *P+S* mode in their numerical simulations of the flow past a cylinder under forced transverse oscillations at Re=500. But the dynamics of the "transverse" P+S mode are different as the transverse oscillations induce a different roll up of the shear layers.

As shown in the fluid force analysis, another transition appears at *A/D*=0.35 via a regain of symmetry. The trajectory of the fluid force is then symmetric every successive cycle of cylinder oscillation. The increase of the amplitude of oscillation results in the formation of a pair and a single vortex every cycle which coalesce in a single vortex downstream in the wake. The result is a *S* vortex wake mode, Figure 10.

Figure 10. Vorticity field (s^{-1}) past an oscillating cylinder in the stream wise direction, A/D=0.35.

Increasing symmetric perturbation of the flow (due to stream wise forced oscillations) induces several transitions in the flow structure as shown by the different resulting vortex wake modes, the fluid force trajectory and the resulting forced Strouhal number. Symmetry breaking of the vortex shedding and period-doubling of the wake flow structure were observed. Ongoren & Rockwell (1988) classified wake patterns found in their experiments into symmetric modes of vortex shedding, asymmetric modes and competition of two

Copyright © 2006 by ASME

modes. In order to explain the supposed symmetry mode competition and the resulting wake, a POD decomposition of the velocity profile was performed to extract the principal spatio-temporal wake structures. The results are presented next.

4. Proper Orthogonal Decomposition (POD)

The POD methodology has already been presented in Mureithi & Rodriguez (2005). POD is a singular value decomposition of the fluctuating velocity profile reducing the wake into its main spatio-temporal modes. Each mode is the product of a temporal component named *chronos* and a spatial one named *topos*. The *chronos* gives the time evolution of the mode while the *topos* gives its shape. Applying POD, on results for *A/D* from 0 to 0.4, gives insight into the symmetry mode competition in the wake.

The decomposition of the flow past the fixed cylinder shows mainly two modes (Figure 11). The first mode containing 99% of the energy of the fluctuating flow have a symmetric *topos* and its *chronos* frequency decomposition gives a main frequency equal to the vortex shedding frequency, f_n. The second mode is composed of an even *topos* and a *chronos* whose principal frequency is at $2f_n$. Higher modes contain less than 0.1% of the fluctuating energy thus it can be concluded that the Karman wake is mainly the sum of the first two modes. This finding is in concordance with the analysis of Williams et al. (1992) where the Karman vortex street was described as the superposition of a sinuous mode at the vortex shedding frequency and a varicose mode at twice the vortex shedding frequency.

POD analysis explores the effect of controlled streamwise excitation. The symmetric oscillations at the fixed cylinder vortex shedding frequency are applied to the Karman vortex street. The latter is characterized as a sinuous mode.

For small amplitudes of oscillation, for *A/D* up to 0.1, the POD decomposition (where only *topos* are shown in Figure 12), shows that the wake contains four modes, the first containing more than 30% of the fluctuating energy, the second close to 20% while the third and fourth contains close to 10% each. The first mode is antisymmetric and the frequency decomposition of its *chronos* has a main frequency close to f_n. The second mode is an even mode whose *chronos* main frequency is close to the forcing frequency. The third and fourth modes have no symmetry in their *topos* and their *chronos* frequency decomposition is more complex than in the two first modes even though their main frequency is close to the forcing frequency. The first mode *topos* has the shape of the fixed cylinder wake main mode *topos* while the symmetric second mode is the result of the streamwise forced oscillations of the cylinder.

For $0.1<A/D<0.125$ (not shown), the first two modes have disturbed *topos* in term of symmetry and a chaotic time evolution of their *chronos*. Two non symmetric modes emerge from the POD decomposition each one containing close to 10% of the fluctuating energy.

For $A/D=0.15$ (not shown), the POD yields two main modes showing a clear harmonic decompositions and symmetries in their *topos*. The wake has recovered a first antisymmetric mode but now at half the fixed cylinder vortex shedding frequency and a second mode, symmetric at the forcing frequency. The effect of forced oscillations is therefore a period doubling of the antisymmetric mode. The first mode has close to 90% of the energy, the second mode slightly over 10%.

For $0.175<A/D<0.325$, Figure 13, the POD decomposition shows that more than 98% of the fluctuating energy is contained in the two first modes. They have no clear symmetry and the frequency decomposition of the *chronos* gives a mixed frequency decomposition of the forcing frequency and the fixed cylinder vortex shedding frequency.

For $A/D=0.35$, Figure 14, the POD decomposition shows that more than 99% of the fluctuating energy is contained in the two first modes. The two modes have the same *topos* as in the case of the fixed cylinder but now frequency decomposition gives the same signal than in the fixed cylinder case but halved in frequency. The frequency decomposition of the second mode *chronos* clearly indicates the forcing frequency of the cylinder. The peak at the forcing frequency is sharper than in the first mode frequency decomposition and the second mode contains 10% of the fluctuating energy.

The POD decomposition shows the results of the forcing as an excitation of the second mode of the Karman wake even at twice the vortex shedding frequency and gives insights into the flow bifurcation behaviour as the amplitude of oscillation of the cylinder is increased. The first significant result is that the Karman vortex street is the sum of an even mode at the vortex shedding frequency and an odd mode at twice the vortex shedding frequency. Low amplitude of forcing slightly perturbs the *2S* mode and results, in the POD, in a period doubling of the second symmetric mode and in the appearance of secondary modes. Increasing the amplitude of oscillations, chaotic vortex shedding is found and non symmetric modes with chaotic *chronos* are extracted via POD. The period-doubling at A/D=0.15 is confirmed by POD and, as shown in the fluid force trajectory, the period-doubling is incomplete. POD shows that it is the second and third modes which seem to have not completed their transition (not shown). The *P+S* mode which results from a symmetry breaking of the wake flow; but having periodic vortex shedding, is found in what has been called the mixed frequency decomposition of *chronos* coupled with non symmetric *topos*. Finally, the *S* mode at A/D=0.35 is exactly the period doubling of the fixed cylinder wake with the same *topos* coupled with oscillations at half the forcing frequency. The period doubling is accomplished by a symmetric forcing via an energy transfer through the second and even mode of the wake flow to odd and main mode characterizing the wake dynamics.

Copyright © 2006 by ASME

CONCLUSIONS

Numerical simulations have been used to investigate the dynamics of the wake flow past a force oscillating cylinder at Re= 1000. The simulations yield the response of the nonlinear Navier Stokes equations to a harmonic streamwise excitation.

Nonlinear responses of the wake have been uncovered including quasi periodic, chaotic responses and period-doubling of the fluid force as the amplitude of oscillation was increased.

Symmetrical forced oscillations were found to have a strong effect on the resulting dynamics of the wake characterized by a periodic vortex shedding. Pitchfork bifurcation via a symmetry breaking of the vortex wake mode giving the *P+S* mode and period-doubling of the vortex wake, leading to the *S* mode, were found. Enhancement of the roll up of the shear layers, as the amplitude of oscillations is increased, explained these transitions in the vortex wake modes.

The Proper Orthogonal Decomposition confirmed a symmetric mode decomposition of the wake flow and explained the effect of the forcing in term of transition in the spatio-temporal modes present in the wake. The mechanism of mode competition leading to the final period-doubling of the wake has been elucidated.

Numerical simulations of the two-dimensional flow using a finite volume method gave insight into the complex dynamics resulting from controlled wake excitation.

REFERENCES

Blackburn, H.M., and R.D. Henderson. 1999. A study of two-dimensional flow past an oscillating cylinder. *J. Fluid Mechanics,* **385**, 255-286.

Blevins, R.D. 1990. Flow-induced vibration, 2nd edition Van Nostran Reinhold, New York, USA.

Griffin, O.N, Ramberg, S.E. 1974. The vortex-street wakes of vibrating cylinders. *Journal of Fluid Mechanics*, **66**, 553-576.

Hua, C., R.P. LeBeau , and P.G. Huang. A Cell-Centered Pressure Based Method for Unstructured Incompressible Navier-Stokes Solvers. *43rd AIAA Aerospace Sciences Meeting and Exhibit, AIAA-2005-0880*, Reno, NV, January 10-13, 2005.

Ongoren, A. and Rockwell, D. 1988. Flow structure from an oscillating cylinder, Part I&II. *Journal of Fluid Mechanics*, **191,** 197-223 and 225-245.

Mureithi, N.W., Kanki, H., Goda, S., Nakamura, T., and Kashikura, T., 2002, Symmetry breaking and mode interaction in vortex-structure interaction, Paper IMECE 2002-32512, *Proceedings, 5th International Symposium on FSI, AE & FIV+N, ASME Int'l Mech. Engrg. Congress & Exhibition*, New Orleans, Louisiana, USA.

Mureithi, N.W., Rodriguez, M. 2005. Stability and bifurcation analysis of a forced cylinder wake. Paper IMECE 2005-79778, *Proceedings, ASME Int'l Mech. Engrg. Congress & Exhibition*, Orlando, Florida, USA.

Nishihira, T., Taneko, S., Watanabe, T. 2005. Characteristics of fluid dynamics forces acting on a circular cylinder oscillated in the streamwise direction and its wake patterns. *Journal of Fluids and Structures,* **20**, 505-518.

Roshko, A., On the Development of Turbulent Wakes from Vortex Sheets. *NACA Report* 1191, 1954.

Van Dyke, M. 1982. An album of fluid motion, *Parabolic Press*.

Williams D.R., Mansy H. and Amato C. 1992. The response and symmetry properties of a cylinder wake subjected to localized surface excitation. *Journal of Fluid Mechanics*, **234,** 71-96.

Williamson C.H.K. and Roshko, A. 1988. Vortex formation in the wake of an oscillating cylinder, *Journal of Fluids and Structures*, **2,** 355-381.

Copyright © 2006 by ASME

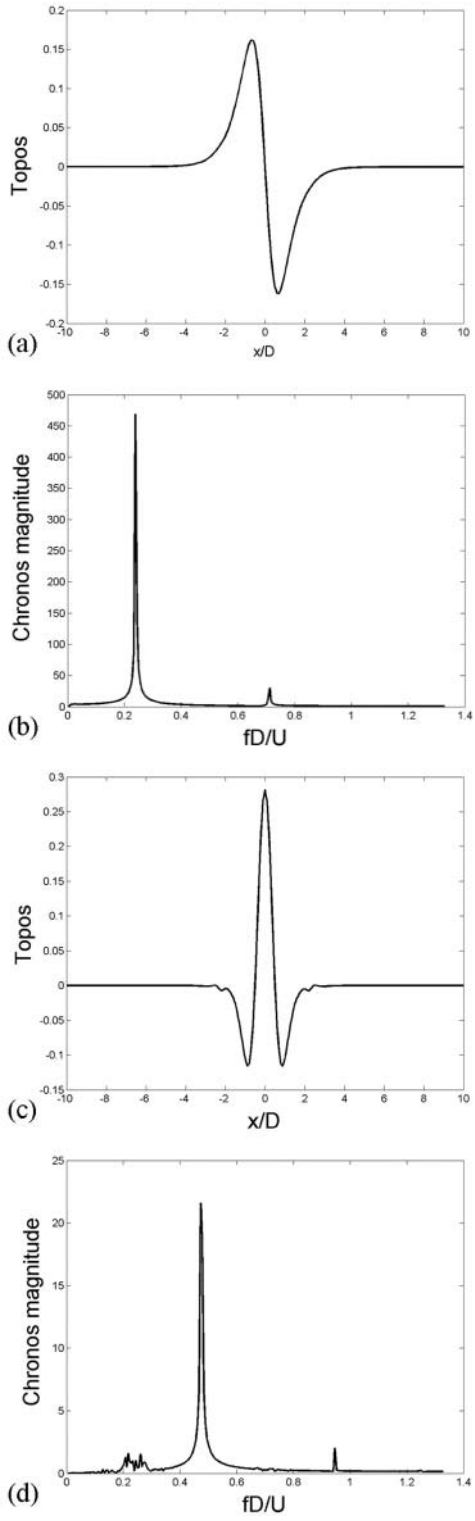

Figure 11. POD decomposition of the wake flow *10D* downstream of the fixed cylinder showing:
First mode (a) topos and (b) chronos. Second mode (c) topos and (d) chronos.

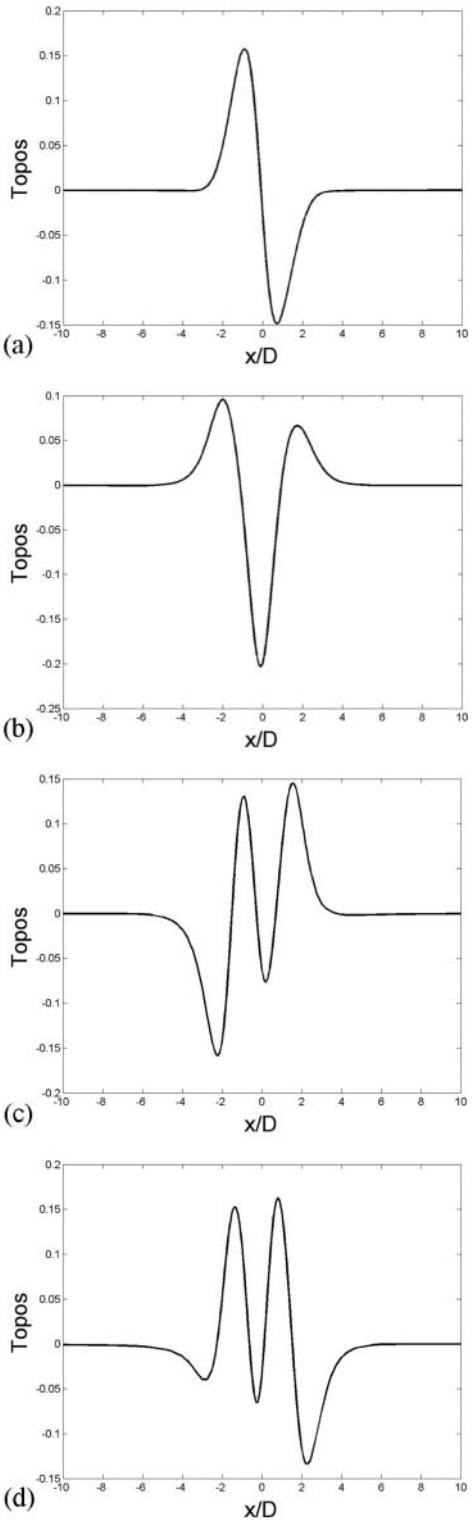

Figure 12. POD decomposition of the wake flow *10D* downstream of the cylinder oscillating at *A/D=0.05* showing:
First (a), second (b), third (c) and fourth (d) modes topos.

Copyright © 2006 by ASME

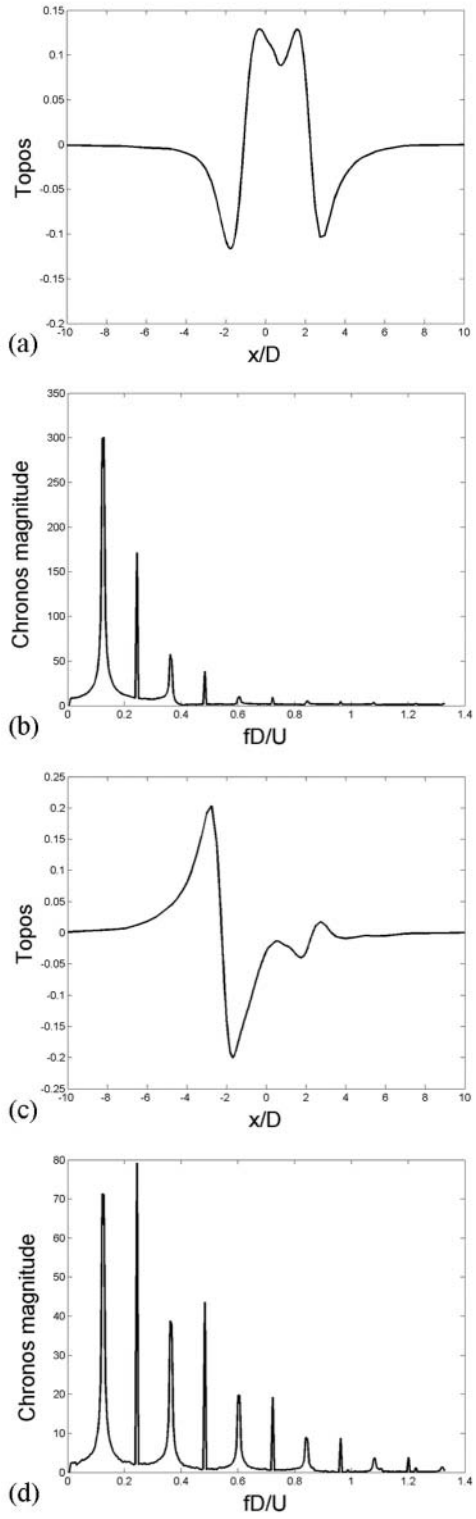

Figure 13. POD decomposition of the wake flow *10D* downstream of the cylinder oscillating at *A/D=0.25* showing: First mode (a) topos and (b) chronos. Second mode (c) topos and (d) chronos.

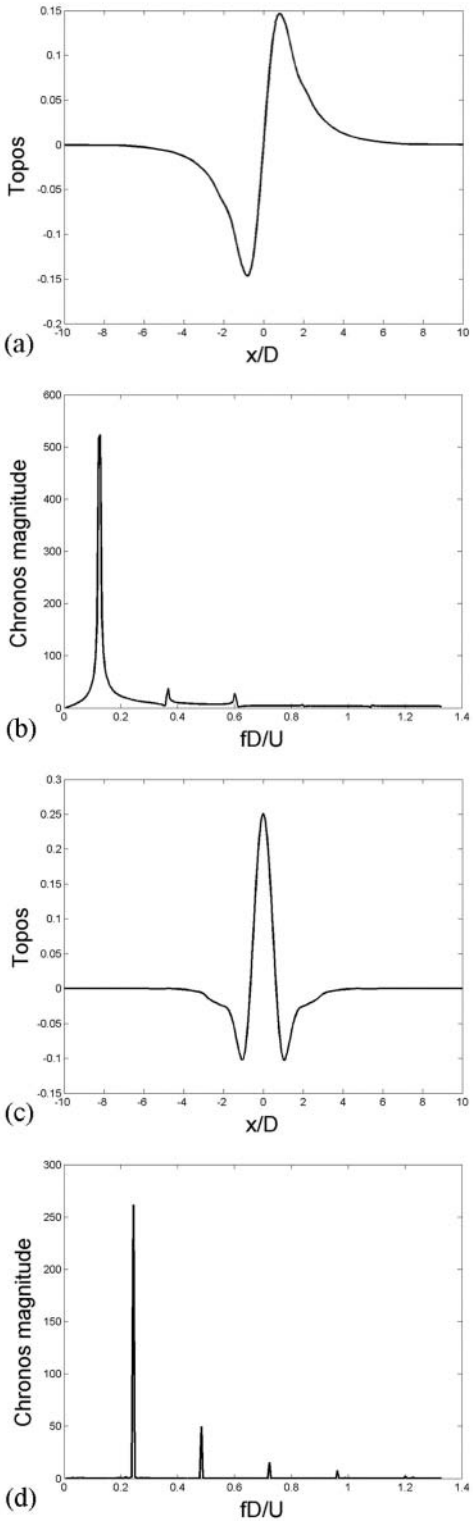

Figure 14. POD decomposition of the wake flow *10D* downstream of the cylinder oscillating at *A/D=0.35* showing: First mode (a) topos and (b) chronos. Second mode (c) topos and (d) chronos.

Copyright © 2006 by ASME